Biointerface Research in Applied Chemistry
Open-Access Journal (ISSN: 2069-5837)

Article
Volume14, Issue 4,2024, 85
https://doi.org/10.33263/BRIAC144.085

Analytical Mathematical Transformation of Correlated Data into Uncorrelated Raman Fiber Spectra for Determination of Nanoparticles of Low-Concentrated Colloidal Silveritle

Viktor M. Emelyanov [1,*], Tatiana A. Dobrovolskaya [1,*], Viktor V. Yemelyanov [1]

[1] The Southwest State University; vmemelianov@yandex.ru (V.M.E); dobtatiana74@mail.ru (T.A.D); wemelyanov@yandex.ru (V.V.E);
* Correspondence: vmemelianov@yandex.ru (V.M.E), dobtatiana74@mail.ru (T.A.D);

ScopusAuthor ID 56344103500

Received: 12.06.2023; Accepted: 11.08.2023; Published: 20.07.2024

Abstract: Analytical forms of multidimensional systems of mathematical transformation equations into uncorrelated form are obtained with their simultaneous solution for equivalent ellipse radii of distributions R0 and R1, as well as probability densities p0 and p1 with the detection of colloidal silver nanoparticles at a concentration of 5% on polyester fibers with multidimensional correlation statistical data of Raman polarization spectra. Analytical forms prove the identification of equations of equivalent radii of ellipses of data spreads when converting them into an uncorrelated form due to the absence of these equations of radii of the mean term, which is present in equations with correlation. The Bayes hypothesis on multiplying non-correlative multidimensional statistical polarization data obtained by transformation in the X and Y directions is used. For a 5% concentration of colloidal silver, the resolution of the identification of silver nanoparticles was obtained by the probability densities of the intersection of the distribution ellipses p0 and p1 up to 10^{-1}-10^{-64}, and by the equivalent radii of the distribution ellipses R0 and R1 up to 0.0304-4.344.

Keywords: multidimensional analysis; correlation equations; colloidal silver nanoparticles; analytical transformation; Raman scattering; recognition reliability; resolution; identification of nanoparticles.

1. Introduction

To ensure the possibilities of nano, pico, and molecular biotechnology research, accuracy and resolution in the range of 10^{-9}-10^{-16} of technical devices and mathematical processing models with an estimate of the probability densities of the intersection of the a priori (initial) and aposteriori (after the experiment) experimental data are necessary [1].

In [2,3], a possible amplification of signals using Raman spectroscopy up to 10^7 using graphene [4-8] and silicon surface vertical nanofibers with a combination of various metal nanoparticles Ag, Au, Cu [9,10] using plasmon effects was revealed. An additional increase in signal amplification up to 10^{10} is possible due to the deposition of graphene or graphene oxide on the surface of metal nanoparticles [11-15].

The most promising method of increasing the resolution is the use of interdependencies (correlations) between multidimensional parameters when processing a large number of statistical data of Raman spectroscopy [16-25]. It is necessary to pay attention to the fact that

there are no independent (uncorrelated) multidimensional parameters in nature, which cannot be neglected. Otherwise, you may lose the credibility of the research.

The use of correlation multidimensional interdependencies in the work [26] revealed the possibility of constructing mathematical models and solving the problem while obtaining accuracy up to 10^{-16}-10^{-18}. But with such high accuracy of solutions of systems of multidimensional equations, the resolution is provided only in the range of 10^{-1}-10^{-7} and is in sufficient to identify nanoparticles with the required resolution of 10^{-16} comparable to the currently obtained accuracy in solving multidimensional correlation mathematical equations.

In the studies of [27], a resolution was obtained for one maximum peak of 10^{-26} in the X, and Y directions. For 9 such peaks, a resolution of up to 10^{-547} was revealed at a high concentration of nanosilver of 17%. However, it is necessary to confirm the resolution on experimental data with a lower concentration of colloidal silver, for example, 5%, following the objectives of this work [27,28]. In addition, it is necessary to prove and show by examples the transformation into an uncorrelated form by the analytical form of the equations of ellipses and multidimensional ellipsoids according to the analytical form of multidimensional statistical data with probabilistic multiplication.

The problems posed in this case are that the compilation and solution of systems of correlation equations require a large number of equations in the system, for example, up to 81. Such a large number of equations is necessary to account for all significant 9 peaks of the Raman spectrum in two directions: across X and along Y of the object of study. Drawing up and solving many correlation equations in a system at this technical level is impossible, even with artificial intelligence. A simplified compilation and solution of the system of these equations does not provide the required reliability.

Applying the Bayes hypothesis on the multiplication of interdependent (correlation) probabilities P_i/P_{ic}, it is possible to obtain the total probability $P_0 = \prod P_i/P_{ic}$ of the occurrence of events [29,30].

However, obtaining interdependent probabilities for many parameters is almost impossible, and it is also challenging to compose and solve a multidimensional system of up to 81 equations. In [26-28], solutions were obtained only for two-dimensional correlation mathematical models and in [31] for three-dimensional ones.

Therefore, to apply the Bayes hypothesis to a large number of parameters, it is necessary to mathematically transform all interdependent (correlation) parameters into an independent (non-correlation) form, and then you can use the Bayes hypothesis for independent probabilities P_i to calculate the total probability of occurrence of independent events $P_0=\prod P_i$.

Research in [26] aims to solve the problem of converting dependent (correlation) data into an independent form and vice versa from independent data into a dependent form. In these studies, the mathematical, analytical transformation into an independent form is performed simultaneously with solving a system of multidimensional correlation equations for a 5% concentration of colloidal silver.

2. Materials and Methods

Textile nanomodified materials, namely polyester fibers, were selected for the study. The results of studies on nanoparticles' effect on textile materials' properties are reflected in [32-36]. Within the framework of this scientific work, analytical methods of mathematical transformation of correlated data into uncorrelated Raman spectra of polyester fibers are proposed.

In general, the analytical equation of an ellipse with dependent (correlation) statistical data when converting the vector-matrix shape of an ellipse used in[28-30] will look like:

$$\left(\frac{x-MENX0_i}{\sigma\Delta X0_i}\quad\frac{y-MENY0_j}{\sigma\Delta Y0_j}\right)\cdot\sum 0^{-1}\cdot\left(\begin{matrix}\frac{x-MENX0_i}{\sigma\Delta X0_i}\\ \frac{y-MENY0_j}{\sigma\Delta Y0_j}\end{matrix}\right)\rightarrow$$

$$\rightarrow\left[\frac{1}{1-\left(rXY0_{i,j}\right)^2}\right]\cdot\left[\frac{\left(x-MENX0_i\right)^2}{\left(\sigma\Delta X0_i\right)^2}-2\cdot\frac{\left(y-MENY0_j\right)}{\sigma\Delta Y)_j}\cdot\frac{\left(x-MENX0_i\right)}{\sigma\Delta X0_i}\cdot rXY0_{i,j}+\frac{\left(y-MENY0_j\right)^2}{\left(\sigma\Delta Y0_j\right)^2}\right],(1)$$

where $\sum 0=\begin{pmatrix}1 & rXY0_{i,j}\\ rXY0_{i,j} & 1\end{pmatrix}$-correlation matrix of the data of the ellipse of the spread of the values of the peaks of the Raman spectrum

Thus, by expression 1, the classical analytical form of the equivalent ellipse radius with correlation $rXY0_{i,j}$ in the middle term of the equation and the general term$1/[1-(rXY0_{i,j})^2]$ is obtained. The accuracy of solving nonlinear equations, in this case for fibers without nanoparticles and with silver nanoparticles, is:

$f(v_0,v_1)=-3.1029760605846133\times10^{-16}$, $g(v_0,v_1)=1.6736919950142115\times10^{-18}$.

The equivalent radii of the ellipses in the solution have the following values:

R0=0.2176497094749659, R1=0.2176497094749652.

The probability density of the intersection of ellipses of data spreads is estimated when solving:

pQ0=0.2708650380340899, pQ1=0.27086503803409023.

To transform this form into a non-correlative form, it is necessary to find the eigenvalues (values) of the correlation matrix ∑0: the basis of the transformation is to obtain from the correlation matrix rXY a diagonal matrix of eigenvalues λ0=eigenvals (rXY) [20].

Finding the diagonal matrix of the eigenvalues of the correlation matrix is mathematically worked out in [29]. For example, for two-dimensional data for the correlation dependence on X and Y, when solving a specific problem of converting Raman spectra in the MathCAD program, we obtain:

1. Drawing up a matrix for the equation of transformation of correlation eigenvalues into non-correlation ones

Given

$$\left|\begin{pmatrix}1-\lambda0 & rXY0_{i,j}\\ rXY0_{i,j} & 1-\lambda0\end{pmatrix}\right|=0 \quad (2)$$

2. Solution of the equation of transformation of correlative eigenvalues into non-correlative ones

$$Find(\lambda0)\rightarrow\left(rXY0_{i,j}+1\quad 1-rXY0_{i,j}\right)(3)$$

3. Construction of a matrix of transformation of correlation eigenvalues into non-correlation ones for the simultaneous solution of a system of the intersection of ellipses without nanoparticles and with nanoparticles without correlation $rXY0_{i,j}$, but with conversion coefficients $1/(1-rXY0_{i,j})$and$1/(1+rXY0_{i,j})$

$$\sum 0:=\begin{pmatrix}1-rXY0_{i,j} & 0\\ 0 & 1+rXY0_{i,j}\end{pmatrix}.(4)$$

4. Construction of a matrix for converting correlative eigenvalues into non-correlative ones with conversion coefficients: $1/(1+rXY0_{i,j})$,$1/(1-rXY0_{i,j})$

$$\sum 0 := \begin{pmatrix} 1 + rXY0_{i,j} & 0 \\ 0 & 1 - rXY0_{i,j} \end{pmatrix} .(5)$$

Then, the transformation of mathematical models with silver nanoparticles and without nanoparticles into an uncorrelated form with simultaneous solution of a system of equations with uncorrelated matrices will have the following form:

$$\frac{(x - MENX0_i)^2}{(1 - rXY0_{i,j}) \cdot (\sigma\Delta X0_i)^2} + \frac{(y - MENY0_j)^2}{(1 + rXY0_{i,j}) \cdot (\sigma\Delta Y0_j)^2} .(6)$$

Here, by expression (4), the classical analytical form of the equivalent ellipse radius without the middle term (3) and, accordingly, without correlation $rXY0_{i,j}$, but with conversion coefficients $1/(1-rXY0_{i,j})$ and $1/(1+rXY0_{i,j})$ for fibers without nanoparticles is obtained.

It is also possible to obtain a classical analytical form of the equivalent ellipse radius without correlation $rXY1_{i,j}$, but with conversion coefficients $1/(1-rXY1_{i,j})$ and $1/(1+rXY1_{i,j})$ for fibers with nanoparticles:

$$\frac{(x - MENX1_i)^2}{(1 - rXY1_{i,j}) \cdot (\sigma\Delta X1_i)^2} + \frac{(y - MENY1_j)^2}{(1 + rXY1_{i,j}) \cdot (\sigma\Delta Y1_j)^2} .(7)$$

The solution of the system of equations (6) and (7) gives the result:

$f(v0,v1)=1.6718992973977542\times10^{-15}$, $g(v0,v1)=-1.7321485059284158\times10^{-20}$;

R0=0.518568257415189, R1=0.5185682574151874;

pQ0=0.21774290198552754, pQ1=0.21774290198552784.

From the results of this solution, it can be seen that in comparison with the unformulated data (1), the accuracy of the solution increases, the radii of the ellipses increase by 2.5 times, and the probability densities of the intersection of the ellipses decrease.

An exciting variant of solving the system of equations (6) and (7) when bound to the axis $MENY0_j=0$– –$MENY1_j=0$ gives the following equations:

$$\frac{(x - MENX0_i)^2}{(1 - rXY0_{i,j}) \cdot (\sigma\Delta X0_i)^2} + \frac{(y - 0)^2}{(1 + rXY0_{i,j}) \cdot (\sigma\Delta Y0_j)^2} .(8)$$

$$\frac{(x - MENX1_i)^2}{(1 - rXY1_{i,j}) \cdot (\sigma\Delta X1_i)^2} + \frac{(y - 0)^2}{(1 + rXY1_{i,j}) \cdot (\sigma\Delta Y1_j)^2} .(9)$$

Expressions (8) and (9) are algebraic expressions of the equivalent radius of the data scattering ellipse for fibers without nanoparticles and with silver nanoparticles, respectively.

The result of solving a system of equations based on (8) and (9) is shown below:

$f(v_0,v_1)=8.820317448412741\times10^{-16}$, $g(v_0,v_1)=0.00000000000000000\times10^{0}$;

R0=0.5146078013008942, R1=0.5146078013008935;

pQ0=0.2510348938835279, pQ1=0.2510348938835278.

The variant of solving the system of equations (8) and (9) concerning the axis $MENY0_j=0$– –$MENY1_j=0$ has a worse result compared to the variant (7) concerning the axis $MENY0_j$– –$MENY1_j$.

The graphic image must also assess the reliability of the intersection of the ellipses of the distribution of the Raman spectra of polyester fibers with silver nanoparticles and without nanoparticles. Graphically, this solution is shown in Figure 1.

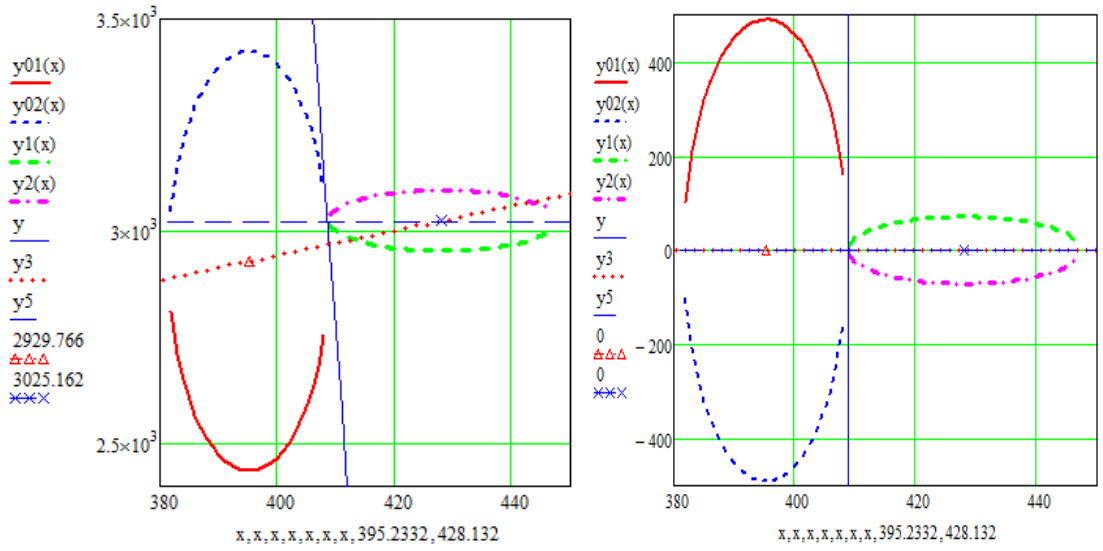

(**a**) (**b**)

Figure1. Validation by graphical representation of the intersection of ellipses of the distribution of Raman spectra of polyester fibers with silver nanoparticles and without nanoparticles: (**a**) graphical representation of the intersection of data distribution ellipses concerning the axis MENY0j– –MENY1j; (**b**) image of ellipses concerning the axis MENY0j=0–-–MENY1j=0.

It is also necessary to check the solution of the system of equations when using conversion coefficients in an uncorrelated form. The analytical form of the ellipses of the data spreads of Raman spectra of polyester fibers with conversion coefficients $1/(1+rXY0_{i,j})$, $1/(1-rXY0_{i,j})$, $1/(1+rXY1_{i,j})$ and $1/(1-rXY1_{i,j})$will have the form:

-without nanoparticles

$$\frac{(x-MENX0_i)^2}{(1+rXY0_{i,j})\cdot(\sigma\Delta X0_i)^2}+\frac{(y-MENY0_j)^2}{(1-rXY0_{i,j})\cdot(\sigma\Delta Y0_j)^2}. \quad (10)$$

-with silver nanoparticles

$$\frac{(x-MENX1_i)^2}{(1+rXY1_{i,j})\cdot(\sigma\Delta X1_i)^2}+\frac{(y-MENY1_j)^2}{(1-rXY1_{i,j})\cdot(\sigma\Delta Y1_j)^2}. \quad (11)$$

The solution of the system of equations (8) and (9) gives the results:

$f(v_0,v_1)=1.3974132254583065\times10^{-15}$, $g(v_0,v_1)=5.26933565110835500\times10^{-20}$;

R0=0.2906458829594823, R1=0.2906458829594799;

pQ0=0.26423016769209184, pQ1=0.2642301676920919,

which is the worst so far, both in accuracy and resolution.

It is also necessary to solve the system of equations using the conversion coefficients in an uncorrelated form: $1/(1-rXY0_{i,j})$, $1/(1-rXY0_{i,j})$, $1/(1-rXY1_{i,j})$ and $1/(1-rXY1_{i,j})$. At the same time, the analytical form of the ellipses of the scatter data of the Raman spectra of polyester fibers will be as follows:

-without nanoparticles

$$\frac{(x-MENX0_i)^2}{(1-rXY0_{i,j})\cdot(\sigma\Delta X0_i)^2}+\frac{(y-MENY0_j)^2}{(1-rXY0_{i,j})\cdot(\sigma\Delta Y0_j)^2}. \quad (12)$$

-with silver nanoparticles

$$\frac{(x-MENX1_i)^2}{(1-rXY1_{i,j})\cdot(\sigma\Delta X1_i)^2}+\frac{(y-MENY1_j)^2}{(1-rXY1_{i,j})\cdot(\sigma\Delta Y1_j)^2}. \quad (13)$$

The solution of the system of equations (12) and (13) gives the results:

$f(v_0,v_1)=-1.7689036243683098\times10^{-15}$, $g(v_0,v_1)=-2.80494816061533260\times10^{-20}$;

R0=0.5535352710448955, R1=0.5535352710448971;

pQ0=0.7926131304595755, pQ1=0.7926131304595752,

which is the worst so far both in accuracy and resolution for p0 and p1.

Finally, it is necessary to solve the system of equations using the conversion coefficients in an uncorrelated form: $1/(1+rXY0_{i,j})$, $1/(1+rXY0_{i,j})$, $1/(1+rXY1_{i,j})$ and $1/(1+rXY1_{i,j})$. The analytical view of the ellipses of the data spreads of the Raman spectra of polyester fibers in this case:

-without nanoparticles

$$\frac{(x-MENX0_i)^2}{(1+rXY0_{i,j})\cdot(\sigma\Delta X0_i)^2}+\frac{(y-MENY0_j)^2}{(1+rXY0_{i,j})\cdot(\sigma\Delta Y0_j)^2}. \quad (14)$$

-with silver nanoparticles

$$\frac{(x-MENX1_i)^2}{(1+rXY1_{i,j})\cdot(\sigma\Delta X1_i)^2}+\frac{(y-MENY1_j)^2}{(1+rXY1_{i,j})\cdot(\sigma\Delta Y1_j)^2}. \quad (15)$$

The solution of the system of equations (14) and (15) gives the results:

$f(v_0,v_1)=-8.749870943297418\times10^{-17}$, $g(v_0,v_1)=-2.18263842823098340\times10^{-21}$;

R0=0.16777092273133723, R1=0.1677709227313375;

pQ0=0.08556173556873917, pQ1=0.08556173556873917,

which is the worst in both accuracy and resolution for R0 and R1.

It is also necessary to confirm the intersections of the distribution ellipses of the Raman spectra of polyester fibers with silver nanoparticles and without nanoparticles with the initial experimental correlated data with the results already obtained for (6) and (7). At the same time, the compilation and solution of a system of nonlinear non-correlation equations in analytical form with conversion coefficients correlated to uncorrelated data for a 5% nanosilver concentration with conversion coefficients $1/(1-rXY0_{i,j})$, $1/(1+rXY0_{i,j})$, $1/(1-rXY1_{i,j})$ and $1/(1+rXY1_{i,j})$ in the MathCAD program will have the form:

i:=0 j:=4

$rXY0_{i,j}=0.813$ $rXY1_{i,j}=0.846$

$$\sum 0:=\begin{pmatrix}1-rXY0_{i,j} & 0\\ 0 & 1+rXY0_{i,j}\end{pmatrix} \quad \sum 1:=\begin{pmatrix}1-rXY1_{i,j} & 0\\ 0 & 1+rXY1_{i,j}\end{pmatrix}$$

$$f(x,y):=\left\|\begin{bmatrix}\frac{(x-MENX0_i)^2}{(1-rXY0_{i,j})\cdot(\sigma\Delta X0_i)^2}+\frac{(y-MENY0_j)^2}{(1+rXY0_{i,j})\cdot(\sigma\Delta Y0_j)^2} & 1\\ \frac{(x-MENX1_i)^2}{(1-rXY1_{i,j})\cdot(\sigma\Delta X1_i)^2}+\frac{(y-MENY1_j)^2}{(1+rXY1_{i,j})\cdot(\sigma\Delta Y1_j)^2} & 1\end{bmatrix}\right\|. \quad (16)$$

$$g(x,y):=\left\|\begin{bmatrix}\frac{(x-MENX0_i)}{(1-rXY0_{i,j})\cdot(\sigma\Delta X0_i)^2} & \frac{(x-MENY0_j)}{(1-rXY0_{1,j})\cdot(\sigma\Delta Y0_j)^2}\\ \frac{(x-MENX1_i)}{(1-rXY1_{i,j})\cdot(\sigma\Delta X1_i)^2} & \frac{(x-MENY1_j)}{(1-rXY1_{i,j})\cdot(\sigma\Delta Y1_j)^2}\end{bmatrix}\right\|.$$

(17)

x:=410 y:=3025

Given

f(x,y) = 0

g(x,y) = 0

v:= Find(x,y) $\quad v = \begin{pmatrix} 408.616185 \\ 3023.747936 \end{pmatrix}$

$f(v_0,v_1)=1.6718992973977542\times10^{-15}$ $\quad g(v_0,v_1)=-1.73214850592841580\times10^{-20}$

$$R0 := \frac{(v_0 - MENX0_i)^2}{(1 - rXY0_{i,j})\cdot(\sigma\Delta X0_i)^2} + \frac{(v_1 - MENY0_j)^2}{(1 + rXY0_{i,j})\cdot(\sigma\Delta Y0_j)^2} .(18)$$

$$R1 := \frac{(v_0 - MENX1_i)^2}{(1 - rXY1_{i,j})\cdot(\sigma\Delta X1_i)^2} + \frac{(v_1 - MENY1_j)^2}{(1 + rXY1_{i,j})\cdot(\sigma\Delta Y1_j)^2} .(19)$$

$R0=0.268913\sqrt{R0} = 0.5185682574\ 15189$

$R1=0.268913\sqrt{R1} = 0.5185682574\ 151874$

The evaluation of the reliability of the results of the compilation and solution of nonlinear non-correlation equations in an analytical form is shown by expressions (16-19), and graphical confirmation is presented in Fig.1a. Here, the graphical representation of the intersection of the distribution ellipses of the Raman spectra of polyester fibers with silver nanoparticles and without nanoparticles is also evaluated using the initial experimental correlated data.

3. Results and Discussion

Solutions of 81 equations of the problem under study for peaks from i=0...8 to j=0...8 mathematically transformed uncorrelated statistical data of Raman spectra of polyester fiber with a concentration of silver nanoparticles of 5% are shown in Fig. 2 and 3:

$$R = \begin{pmatrix} 0.52 & 0.463 & 0.363 & 0.486 & 0.349 & 0.626 & 0.106 & 0.499 & 0.298 \\ 0.483 & 0.445 & 0.349 & 0.436 & 0.355 & 0.588 & 0.117 & 0.451 & 0.282 \\ 0.564 & 0.49 & 0.39 & 0.538 & 0.34 & 0.695 & 0.102 & 0.529 & 0.331 \\ 0.493 & 0.454 & 0.352 & 0.456 & 0.368 & 0.601 & 0.121 & 0.465 & 0.292 \\ 0.515 & 0.479 & 0.339 & 0.418 & 0.342 & 1.642 & 0.256 & 0.459 & 0.25 \\ 0.535 & 0.477 & 0.379 & 0.501 & 0.348 & 0.662 & 0.108 & 0.502 & 0.318 \\ 0.501 & 0.476 & 0.33 & 0.423 & 0.368 & 1.587 & 0.291 & 0.459 & 0.253 \\ 0.26 & 0.314 & 0.467 & 0.449 & 0.218 & 0.491 & 0.03 & 0.258 & 0.143 \\ 0.508 & 0.538 & 0.362 & 0.34 & 0.237 & 0.616 & 0.191 & 0.453 & 0.26 \end{pmatrix}$$

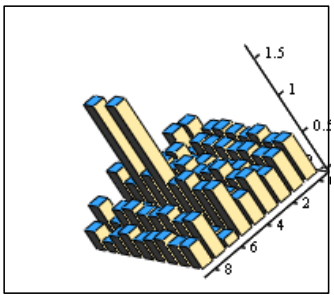

R

Figure 2. Matrix of equivalent intersection radii of ellipses of the distribution of Raman spectra of polyester fibers with a concentration of 5% silver nanoparticles detected by statistical data converted to uncorrelated form.

4. Conclusions

In studies, the obtained analytical forms prove the identification of equations of equivalent radii of ellipses of data spreads without correlation in these equations of radii of the absence of the mean term, which is present in equations with correlation. This is the proof of the correctness of the transformation of correlation statistical data into an uncorrelated form while simultaneously solving a system of equations.

The mathematical method of converting correlation statistical data into uncorrelated form while simultaneously solving a system of equations of multidimensional Raman spectra of polyester fibers without nanoparticles and with silver nanoparticles allows increasing the sensitivity of identification of silver nanoparticles up to 10^{64} times and, consequently, increasing the resolution of the method for 5% concentration of silver nanoparticles.

$$Q = \begin{pmatrix} 5.242 & 6.342 & 6.189 & 5.71 & 6.157 & 5.454 & 6.536 & 5.907 & 6.554 \\ 5.242 & 6.326 & 6.253 & 5.7 & 6.182 & 5.419 & 6.78 & 5.849 & 6.796 \\ 5.137 & 6.364 & 6.066 & 5.723 & 6.225 & 5.396 & 6.505 & 5.968 & 6.357 \\ 5.127 & 6.315 & 6.206 & 5.604 & 6.195 & 5.331 & 6.886 & 5.934 & 6.724 \\ 3.984 & 5.731 & 5.162 & 4.451 & 6.384 & 12.919 & 9.088 & 6.453 & 7.724 \\ 5.121 & 6.344 & 6.088 & 5.605 & 6.23 & 5.351 & 6.652 & 5.978 & 6.453 \\ 4.04 & 5.737 & 5.17 & 4.484 & 6.329 & 12.224 & 9.533 & 6.449 & 7.664 \\ 6.288 & 6.467 & 7.463 & 7.561 & 6.386 & 7.584 & 6.288 & 6.444 & 6.664 \\ 4.494 & 6.162 & 5.905 & 5.388 & 6.279 & 4.833 & 8.089 & 6.221 & 8.359 \end{pmatrix}$$

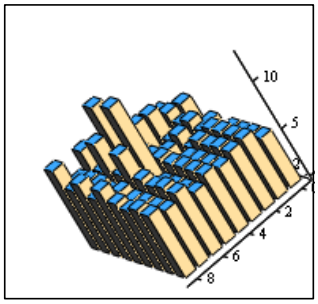

Q

Figure 3. Matrix of confidence in the intersection of ellipses of the distribution of Raman spectra of polyester fibers with a concentration of 5% silver nanoparticles and without nanoparticles.

The equivalent radii of the intersection of the ellipses of the distribution of the Raman spectra of polyester fibers are shown in Figure 4. :

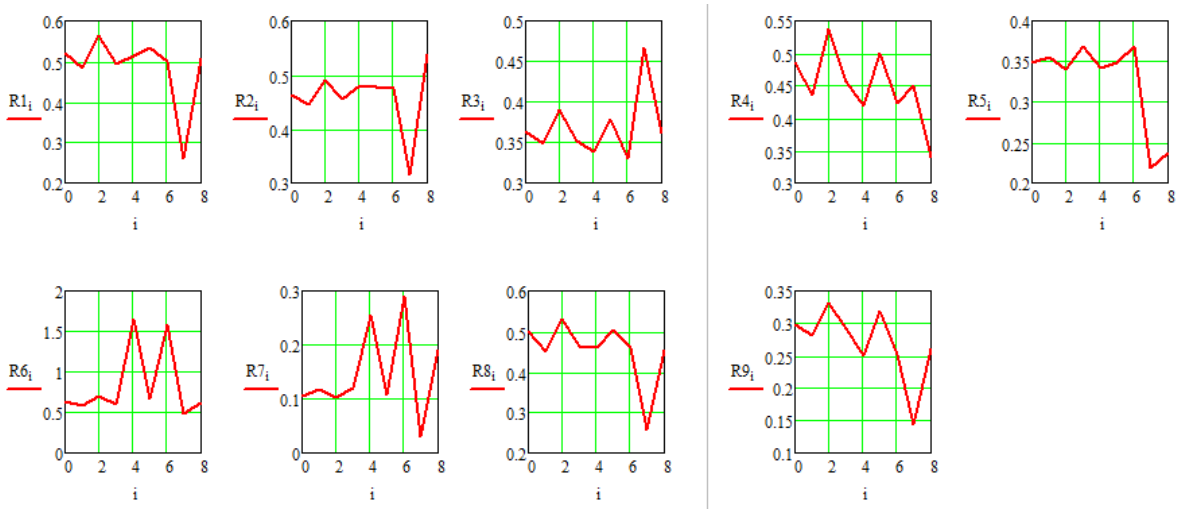

Figure 4. Equivalent radii of the intersection of ellipses of the distribution of Raman spectra of polyester fibers with a concentration of 5% silver nanoparticles in columns j=0-8 of the data matrix R.

The developed method uses the possibilities of applying the Bayes hypothesis when multiplying probability densities at the intersection of the ellipses of the distribution of the values of the peaks of the Raman spectra of polyester with silver nanoparticles and without nanoparticles for transformed uncorrelated data. The translation of correlated statistical data into an uncorrelated form is carried out from the diagonal matrices by the eigenvalues (numbers) of correlation matrices used simultaneously to compile and solve systems of equations.

As a result of the research, we obtained a classical analytical form of the equivalent ellipse radius with correlation rXY0i,j in the middle term of the equation and the general term 1/[1-(rXY0i,j)2].

The accuracy of solving nonlinear equations for fibers without nanoparticles and with silver nanoparticlesis: $f(v_0,v_1) = -3.1029760605846133\times10^{-16}$, $g(v_0,v_1) = 1.6736919950142115\times10^{-18}$.

The equivalent radii of the ellipses in the solution have the values: R0=0.2176497094749659, R1=0.2176497094749652.

The probability density of the intersection of the ellipses of the data spreads is estimated in the solution: pQ0=0.2708650380340899, pQ1=0.27086503803409023.

The solution of a system of equations with an analytical transformation into an uncorrelated form with conversion coefficients of the system of equations $1/(1-rXY0_{i,j})$, $1/(1+rXY0_{i,j})$, $1/(1-rXY1_{i,j})$ and $1/(1+rXY1_{i,j})$ gives the result:

$f(v_0,v_1)=1.6718992973977542\times10^{-15}$, $g(v_0,v_1)=-1.7321485059284158\times10^{-20}$;

R0=0.518568257415189, R1=0.5185682574151874;

pQ0=0.21774290198552754, pQ1=0.21774290198552784.

From the results of this solution, it can be seen in comparison with the uneducated data that the accuracy of the solution increases, the radii of the ellipses increase by 2.5 times, and the probability densities of the intersection of the ellipses decrease.

A system of equations has also been compiled and solved for the mathematical, analytical transformation of two–dimensional dependent (correlation) data into non–correlation data for fibers with and without nanoparticles concerning the axis $MENY0_j=0$ - - $MENY1_j=0$ ellipses of distributions. The results of solving a system of equations when attached to the axis $MENY0_j=0$ – – MENY1j=0 have a worse outcome than the option without binding.

The compilation and solution of systems of equations with analytical transformation into uncorrelated form in different combinations with conversion coefficients: $1/(1-rXY0_{i,j})$ and $1/(1-rXY1_{i,j})$, as well as with conversion coefficients $1/(1+rXY0_{i,j})$ and $1/(1+rXY1_{i,j})$. These results give the worst and most ambiguous values so far.

A matrix of all 81 Q-factor values Q and log Q was also obtained and investigated. Since when multiplying all the independent terms of the matrix Q, we get $10^{64.1}$, i.e., within the computational capabilities of a conventional computer, we can use multiplication of all the values of the terms of the matrix Q. And in the case of the log Q matrix, the addition of all the values of the terms is performed, and the sum value of 64.1 is obtained. For one member of this matrix, we get an average value of 0.791 or $10^{0.791}=6.1802$.

For further research, it is necessary to compile and solve a system of equations for converting correlated data into uncorrelated ones for 11% of the concentration of deposited colloidal silver when compared with 5% and 17% of the already proven research method in this work.

Funding

This research received no external funding.

Acknowledgments

This research has no acknowledgment.

Conflicts of Interest

The authors declare no conflict of interest.

References

1. Hachenberger, Y.U.; Rosenkranz, D.; Kromer, C.; Krause, B.C.; Dreiack, N.; Kriegel, F.L.; Koz'menko, E.; Jungnickel, H.; Tentschert, J.; Bierkandt, F.S.; Laux, P.; Panne, U.; Luch, A. Nanomaterial Characterizationin

Complex Media—Guidanceand Application. *Nanomaterials* **2023**, *13*, 922, https://doi.org/10.3390/nano13050922.
2. Zhou, J.; Zhou, P.-L.; Shen, Q.; Ahmed, S.A.; Pan, X.-T.; Liu, H.-L.; Ding, H-L.; Li, J.;Wang, K.; Xia, X.-H. Probing Multidimensional Structural Information of Single Molecules Transporting through a Sub-10 nm Conical Plasmonic Nanoporeby SERS. *Anal. Chem.* **2021**, *93*, 11679–11685, https://doi.org/10.1021/acs.analchem.1c00875.
3. Kartashova, A.D.; Gonchar, K.A; Chermoshentsev, D.A; Alekseeva, E.A.; Gongalsky, M.B.; Bozhev, I.V.; Eliseev, A.A.; Dyakov, S.A.; Samsonova, J.V.; Osminkina, L.A. Surface-Enhanced Raman Scattering-Active Gold-Decorated Silicon Nanowire Substrates for Label-Free Detection of Bilirubin. *ACS Biomater. Sci.Eng.* **2022**, *8*, 4175–4184, https://doi.org/10.1021/acsbiomaterials.1c00728.
4. Daoudi, K.; Gaidi, M.; Columbus, S. Silvernanoprisms/grapheneoxide/silicon nanowires composites for R6G surface-enhanced Raman spectroscopy sensor. *Biointerface Res. Appl. Chem.* **2020**, *10*, 5670–5674, https://doi.org/10.33263/BRIAC103.670674.
5. Voznyakovskii, A.; Vozniakovskii, A.; Kidalov, S. New Way of Synthesis of Few-Layer Graphene Nanosheets by the Self Propagating High-Temperature Synthesis Method from Biopolymers. *Nanomaterials* **2022**, *12*, 657, https://doi.org/10.3390/nano12040657.
6. Dong, G.; Ding, S.; Peng, Y. Ultraviolet-Sensitive Properties of Graphene Nanofriction. *Nanomaterials* **2022**, *12*, 4462, https://doi.org/10.3390/nano12244462.
7. Zhang, X.; Chen, Z.; Lu, L.; Wang, J. Molecular Dynamics Simulations of the Mechanical Properties of Cellulose Nanocrystals-Graphene Layered Nanocomposites. *Nanomaterials* **2022**, *12*, 4170, https://doi.org/10.3390/nano12234170.
8. Saleem, H.; Goh, P.S.; Saud, A.; Khan, M.A.W.; Munira, N.; Ismail, A.F.; Zaidi,S.J. Graphene Quantum Dot-Added Thin-Film Composite Membrane with Advanced Nano fibrous Support for Forward Osmosis. *Nanomaterials* **2022**, *12*, 4154, https://doi.org/10.3390/nano12234154.
9. Rahman, L.; Shah, A.H.A.; Shah, A.; Salman, S.M.; Jan, A.K. Synthesis and Spectroscopic Analysis of Au-Ag Alloy Nanoparticles with Different Composition of Au and Ag. *Biointerface Res. Appl. Chem.* **2022**, *12*, 377-390,https://doi.org/10.33263/BRIAC121.377390.
10. Radhakrishnan, S.; Sumathi, C.; Dharuman,V.; Wilson, J. Gold nanoparticles functionalized poly (3,4-ethylenedioxythiophene) thin film for highly sensitive label free DNA detection. *Anal.Methods* **2013**, *5*, 684-689, https://doi.org/10.1039/C2AY26143J.
11. Scaglione, F.; Battezzati, L.; Rizzi, P. Breaking Down SERS Detection Limit: Engineering of a Nanoporous Platform for High Sensing and Technology. *Nanomaterials* **2022**, *12*, 1737, https://doi.org/10.3390/nano12101737.
12. Li,W.; Zhou, J.; Maccaferri, N.; Krahne, R.; Wang, K.; Garoli,D. Enhanced Optical Spectroscopy for Multiplexed DNA and Protein-Sequencing with Plasmonic Nanopores: Challengesand Prospects. *Anal.Chem.* **2022**, *94*, 503–514, https://doi.org/10.1021/acs.analchem.1c04459.
13. Khinevich, N.; Zavatski, S.; Kholyavo, V.; Bandarenka, H. Bimetallic nanostructures on porous silicon with controllable surface plasmon resonance. *Eur.Phys.J.Plus*. **2019**, *134*, 75, https://doi.org/10.1140/epjp/i2019-12567-4.
14. Agustina, E.; Goak, J.C.; Lee, S.; Kim, Y.; Hong, S.C.; Seo, Y.; Lee, N. Effect of Graphite Nanoplatelet Sizeand Dispersionon the Thermaland Mechanical Properties of Epoxy-Based Nanocomposites. *Nanomaterials* **2023**, *13*, 1328, https://doi.org/10.3390/nano13081328.
15. Yang, Z. ;Zhang, D.; Wang, K.; He, J.; Li, J.; Huang, C. Investigating graphdiyne based materials for rechargeable batteries. *NanoToday* **2022**, *46*,101588, https://doi.org/10.1016/j.nantod.2022.101588.
16. Rani, C.; Tanwar, M.; Ghosh, T.; Kandpal, S.; Pathak, D.K.; Chaudhary, A.; Yogi, P.; Saxena, S.K.; Kumar, R. Raman. Spectroscopy as a Simple ye tEffective Analytical Tool for Determining Fermi Energy and Temperature Dependent Fermi Shiftin Silicon. *Anal.Chem.* **2022**, *94*,1510–1514, https://doi.org/10.1021/acs.analchem.1c03624.
17. Xu, X; Lin,J.; Guo, Y.;Wu, X.; Xu, Y.; Zhang, D.; Zhang, X.; Yujiao, X.; Wang, J.; Yao, C.; Yao, J.; Xing, J.; Cao, Y.; Li, Y.; Ren, W.; Chen, T.; Ren, Y.; Wu, A. TiO_2-based Surface-Enhanced Raman Scattering bio-probe for efficient circulating tumor cell detection on microfilter. *Biosens. Bioelectron.* **2022**, *210*, 114305, https://doi.org/10.1016/j.bios.2022.114305.
18. Hu, X.; Lo, T.W.; Mancini, A.; Gubbin, C.R.; Martini, F.; Zhang, J.; Gong, Z.; Politi, A.; De Liberato, S.; Zhang, X.; Lei, D.; Maier, S.A. Near-field nano-spectroscopy of strong mode coupling in phonon-polaritonic crystals. *Appl. Phys.Rev.* **2022**, *9*, 021414, https://doi.org/10.1063/5.0087489.

19. Garming, M.W.H.; Weppelman, I.G.C.; Lee, M.; Stavenga, T.; Hoogenboom, J.P. Ultrafast scanning electron microscopy with sub-micrometer optical pump resolution. *Appl. Phys. Rev.* **2022**, *9*, 021418, https://doi.org/10.1063/5.0085597.
20. Li, W.; Zhou, J.; Maccaferri, N.; Krahne, R.; Wang, K.; Garoli, D. Enhanced Optical Spectroscopy for Multiplexed DNA and Protein-Sequencing with Plasmonic Nanopores: Challenges and Prospects. *Anal.Chem.* **2022**, *94*, 503–514, https://doi.org/10.1021/acs.analchem.1c04459.
21. Emelyanov, V.M.; Dobrovolskaya, T.A.; Emelyanov, V.V. Multidimensional system of equations with XY-Y differentiation of probability densities p0-p1 for identification of gold nanoparticles. *Biointerface Res. Appl. Chem.* **2018**, *8* , 3652-3656.
22. Zeng, S.; Li, C.; Huang, L.; Chen, Z.; Wang, P.; Qin, D.; Gao, L. Carbon Nanotube-Supported Dummy Template Molecularly Imprinted Polymers for Selective Adsorption of Amide Herbicides in Aquatic Products. *Nanomaterials* **2023**, *13*, 1521, https://doi.org/10.3390/nano13091521.
23. Kontou, E.; Christopoulos, A.; Koralli, P.; Mouzakis, D.E. The Effect of Silica Particle Sizeonthe Mechanical Enhancement of Polymer Nanocomposites. *Nanomaterials* **2023**, *13*, 1095, https://doi.org/10.3390/nano13061095.
24. Sealy, C. Wrapping carbon nanotubes makes a positive difference to cellular uptake. *NanoToday* **2022**, *47*, 101679, https://doi.org/10.1016/j.nantod.2022.101679.
25. Hu, H.; Shi, F.; Tieu, P.; Fu, B.; Tao, P.; Song, C.; Shang, W.; Pan, X.; Deng, T.; Wu, J. Quasi/non-equilibrium state in nanobubble growtht rajectory revealed by *in-situ* transmission electron microscopy. *NanoToday* **2023**, *48*,101761, https://doi.org/10.1016/j.nantod.2023.101761.
26. Emelyanov,V.M.; Dobrovolskaya,T.A.; Emelyanov,V.V. Mathematical Transformation of Multidimensional Correlated Data into Uncorrelated RamanSpectra to Increase the Sensitivity of Identification with Silver Nanoparticles. *Biointerface Res. Appl. Chem.* **2023**, *13*, *139*, https://doi.org/10.33263/BRIAC132.139.
27. Emelyanov, V.M.; Dobrovolskaya, T.A.; Emelyanov, V.V. Automatic Solution of the System of Equations of the Equivalent Radius of the Distribution Ellipses of Dielectric Materials for the Recognition of Gold Nanoparticles. Proceedings of the International Seminar on Electron Devices Design and Production (SED), Prague, Czech Republic, 27-28 April 2021; Publisher IEEE Xplore, **2021**, 20800604, https://doi.org/10.1109/SED51197.2021.9444524.
28. Emelyanov, V.M.; Dobrovolskaya, T.A.; Emelyanov, V.V. Solution of multidimensional system with XY differentiation of probability density equations fo ridentification of silver nanoparticles on fibers. *IOP Conf.Ser.:Mater.Sci. Eng.* **2020**, *905*, 012014, https://doi.org/10.1088/1757-899X/905/1/012014.
29. Santos-Fernandez, E.; VerHoef, J.M.; Peterson, E.E.; McGree, J.; Isaa, D.J.; Mengersen, K. Bayesian spatio-temporal models for stream networks. *NanoToday* **2022**, *170*, 107446, https://doi.org/10.1016/j.csda.2022.107446.
30. Osei, P.P.; Davidov, O. Bayesian linear models for cardinal paired comparison data. *NanoToday* **2022**, *172*, 107481, https://doi.org/10.1016/j.csda.2022.107481.
31. Emelyanov,V.M.; Dobrovolskaya, T.A.; Emelyanov,V.V. Three-dimensional Differential XYZ-Y Model for Processing Peasurements of Raman Spectra in the Identification of Gold Nanoparticles on Dielectrics. Proceedings of the Moscow Workshopon Electronic and Networking Technologies (MWENT), Moscow, Russia, 1-5 March 2020; Publisher: IEEEXplore, **2020**, 19587807,https://doi.org/10.1109/MWENT47943.2020.9067452.
32. Vasilev, K. Antibacterial Applications of Nanomaterials. *Nanomaterials* **2023**, *13*, 1530, https://doi.org/10.3390/nano13091530.
33. Cuberes, T. Preparation and Application of Polymer Nanocomposites. *Nanomaterials* **2023**, *13*, 657, https://doi.org/10.3390/nano13040657.
34. Wang, C.; Zhang, W.; Xu, X.; Su, J.; Shi, J.; Amin, M.A.; Zhang, J.; Yamauchi,Y. Multifunctional wearable thermal management textile fabricated by one-step sputtering. *NanoToday* **2022**, *45*, 101526, https://doi.org/10.1016/j.nantod.2022.101526.
35. Wang, Y.; Liu, K.-K.; Zhao,W.-B.; Sun, J.-L.; Chen, X.-X.; Zhang, L.-L.; Cao, Q.; Zhou, R.; Dong, L.; Shan, C.-X. Antibacterial fabrics based on synergy of piezoelectric effect and physical interaction. *NanoToday* **2023**, *48*, 101737, https://doi.org/10.1016/j.nantod.2022.101737.
36. Bao, L.; Cui, X.; Mortimer, M.; Wang, X.; Wu, J.; Chen, C. The renaissance of one-dimensional carbon nanotubes in tissue engineering. *NanoToday* **2023**, *49*, 101784, https://doi.org/10.1016/j.nantod.2023.101784.